DOI: 10.61782/fa.2023.0466

forum acusticum 2023

RADIATION IMPEDANCE CONTROL OF BRASS RESONATORS TO RESHAPE SOUNDS WITH VOWEL SPECTRAL ENVELOPES: A NUMERICAL STUDY

Vincent Martos[1,2*] **Henri Boutin**[1,2] **Thomas Hélie**[2]
Brigitte d'Andréa-Novel[1,2]
[1] Sorbonne Université, Paris, France
[2] S3AM-STMS-Ircam, Sorbonne Université, 1, place Igor Stravinsky, 75004 Paris, France

ABSTRACT

The application of active control to brass instruments brings many benefits to composers and performers, by expanding its sound possibilities. In this paper, we propose to simulate the connection of a static human vocal tract, downstream of the bell, so that the instrument radiates a vowel. To this end, we modulate the spectral envelope of the radiated sound by a series of formants, namely the vocal tract resonances.

Using source-filter modeling and the laws of linear acoustics, this amounts to introducing the transfer function of the vocal tract between the resonator and the natural radiation impedance of the instrument. The vocal tract model is a succession of straight tubes of constant cross-sectional areas, cascaded using the transfer matrix method.

For this purpose, a controller is introduced in a feedback loop. It takes as input the acoustic pressure measured by a microphone at the bell and calculates the contribution to be added to the natural flow rate out of the bell to obtain the target flow. The actuator consists of several loudspeakers co-located with the microphone.

The control is validated by successively simulating several target vocal tracts and by quantifying the variations of the spectral envelope of the radiated sound.

*__Corresponding author__: vincent.martos@ircam.fr.

Keywords: *Active control, Augmented brass instrument, Formants*

1. INTRODUCTION AND PROBLEM STATEMENT

The objective of the paper is to create an *augmented* trombone, aiming to widen the potentialities of the interpreter's playing modes without changing the correlation between auditory feedback (what he hears) and haptic feedback (what he feels via his lips). Specifically, we propose to use active control to apply a formant envelope to the radiation impedance of the trombone, thus allowing the performer to modulate the natural sounds with human vowels [1]. Such a method is different from an external audio effect that would not take into account the modification of the sensation of the vibration of the lips. The operation of the trombone is described in Fig. 1. The lips of the performer

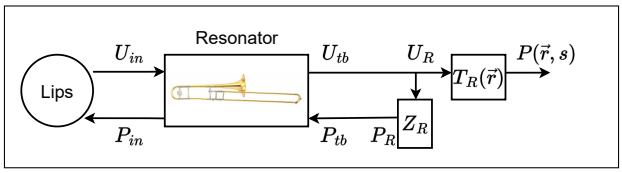

Figure 1. Description of the trombone, acoustic variables and conventions. The flow is counted positively when it occurs from the mouth to the bell.

vibrate at the mouthpiece of the resonator and create an acoustic wave from the mouthpiece to the bell of the trombone (flow U_{in}, pressure P_{in}). At the further end of the bore we represent the radiation by the impedance which

loads the instrument (defined in the Laplace domain by the quotient $Z_R = \frac{P_R}{U_R}$). The transfer function between the output flow rate of the trombone and the pressure at a point $\vec{r}$ of space is noted $T_R(s, \vec{r})$.

In section 2, we present the different models chosen for the trombone, the radiation and the vocal tract. The working hypothesis are exposed too. Then, sections 3 and 4 respectively describe the control structure applied to the radiation impedance, and its implementation using electroacoustic transducers. Finally, section 5 simulates the model of trombone with and without control, successively driven with a chirp signal and a real measurement of mouthpiece flow rate. The obtained input and radiation impedances are compared with theoretical results calculated by FFT.

2. MODELLING

In the following, the trombone, while played, is described in three parts (see Fig. 2): (a) the excitation part (localised at the musician's lips), (b) the acoustic propagation inside the instrument (mouthpiece and bore), and (c) the acoustic radiation (acoustic load at the bell extremity and propagation in the outside domain).

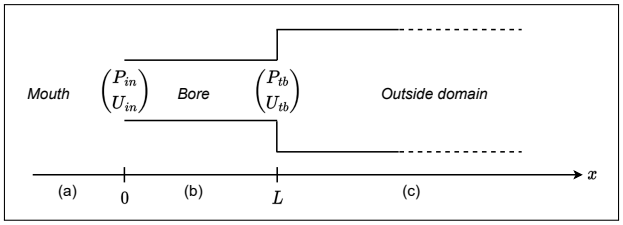

Figure 2. Trombone modelling.

To concentrate on the control issue of the acoustic part (b-c) with the simplest formulae, we consider an oversimplified modelling, namely, conservative planar waves in (see Fig. 2) a single straight pipe for (b) and a semi-infinite (large) straight pipe for (c).
In the same perspective, the effect of the vocal tract, intended to be applied to the radiation impedance, is modelled by an all-pole resonant filter with 4 formants.
All these elements are described below in the Laplace and Z domains.

2.1 Acoustic transfer matrix of a straight pipe T_{tb}

We choose to model the bore of the trombone by a cylinder of cross-section area S_c and length L, represented by the transfer matrix $\tilde{T}_{tb}$ in the Laplace domain and T_{tb} in the Z-domain, which relates the output acoustic state $X_{out} = \begin{bmatrix} P_{tb} \\ U_{tb} \end{bmatrix}$ to the input $X_{in} = \begin{bmatrix} P_{in} \\ U_{in} \end{bmatrix}$ as $X_{out} = \tilde{T}_{tb} X_{in}$, where

$$\tilde{T}_{tb}(s) = \begin{bmatrix} \cosh \frac{s\,L}{c_0} & -Z_c \sinh \frac{s\,L}{c_0} \\ -Z_c^{-1} \sinh \frac{s\,L}{c_0} & \cosh \frac{s\,L}{c_0} \end{bmatrix}, \quad \text{(1a)}$$

for all Laplace variable $s \in \mathbb{C}_0^+ = \{s \in \mathbb{C}\,\text{s.t.}\,\Re e(s) > 0\}$, and where $Z_c = \rho_0 c_0 / S_c$ denotes the characteristic impedance of the pipe (see e.g. [2]). For a sampling rate f_s, the corresponding exact Z-transform is

$$T_{tb}(z) = \begin{bmatrix} \frac{z^N + z^{-N}}{2} & -Z_c \frac{z^N - z^{-N}}{2} \\ -Z_c^{-1} \frac{z^N - z^{-N}}{2} & \frac{z^N + z^{-N}}{2} \end{bmatrix}, \quad \text{(1b)}$$

for all $z \in \mathbb{D} = \{s \in \mathbb{C}\,\text{s.t.}\,|z| < 1\}$, so that $\tilde{T}_{tb}(s) = T_{tb}\big(z = e^{s/f_s}\big)$, and where the delay $N = L f_s / c_0$ is chosen to be integer for simulations below.

2.2 Radiation impedance Z_R and propagation transfer T_R

We choose to model the external environment by a semi-infinite pipe, so that the radiation impedance load is the characteristic impedance of this pipe

$$\tilde{Z}_R \equiv Z_R = \frac{\rho_0 c_0}{S_R}, \quad \text{(2)}$$

and the pressure of the (forward) wave at a point $x \geq L$ is

$$P(s, x) = \tilde{T}_R(s, x) U_{tb}(s), \quad \text{(3a)}$$

$$\text{with } \forall s \in \mathbb{C}_0^+, \quad \tilde{T}_R(s, x) = Z_R\, e^{-s(x-L)/c_0}, \quad \text{(3b)}$$

$$\text{so that } \forall z \in \mathbb{D}, \quad T_R(z, x) = Z_R\, z^{-M(x)}, \quad \text{(3c)}$$

with delay $M(x) = (x - L) f_s / c_0 > 0$, and where $S_R > S_c$ is the pipe cross-section (see Fig. 2).

2.3 Input impedance $Z_{in}^{\emptyset}$ (without control)

The input state X_{in} of the pipe (T_{tb}) loaded by the radiation (Z_R) is related to the acoustic flow at the bell U_R as $X_{in} = T_{tb}^{-1} \begin{bmatrix} Z_R \\ 1 \end{bmatrix} U_R$, from which the input

impedance $Z_{in} = P_{in}/U_{in}$ is derived as

$$\forall s \in \mathbb{C}_0^+, \quad \tilde{Z}_{in}^{\emptyset}(s) = Z_c \frac{\tanh \frac{s\,L}{c_0} + \theta}{1 + \theta \tanh \frac{s\,L}{c_0}}, \tag{4a}$$

$$\forall z \in \mathbb{D}, \quad Z_{in}^{\emptyset}(z) = Z_c \frac{(1+\theta)z^N + (\theta-1)z^{-N}}{(1+\theta)z^N + (1-\theta)z^{-N}}, \tag{4b}$$

with $\theta = \frac{Z_R}{Z_c} = \frac{S_c}{S_R} \in (0,1)$. Their poles are complex conjugated and given by

$$\forall n \in \mathbb{N}, \qquad s_n^{\pm} = -\xi \pm 2i\pi f_n, \tag{5a}$$

$$\forall n \in [1, N]_{\mathbb{N}}, \qquad z_n^{\pm} = \rho\, e^{\pm i\omega_n}, \tag{5b}$$

with $\xi = \frac{c_0}{2L} \ln \frac{1-\theta}{1+\theta} > 0$, $f_n = \frac{(2n+1)c_0}{4L} > 0$, $\rho = \left(\frac{1-\theta}{1+\theta}\right)^{\frac{1}{2N}} \in (0,1)$ and $\omega_n = \frac{(2n+1)\pi}{2N} > 0$). Note that, consistenly, $\rho \equiv e^{-\xi/f_s}$ and $\omega_n \equiv 2\pi f_n/f_s\ [2\pi]$. Note also that the resonance frequencies are given by $f_n^{res} = |s_n^{\pm}|/(2\pi) = f_n\sqrt{1 + \left(\frac{\xi}{2\pi f_n}\right)^2}$ and that the quality factors are $Q_n = |s_n^{\pm}|/(2\xi) = \sqrt{\xi^2 + 4\pi^2 f_n^2}/(2\xi)$.

2.4 Vocal tract H_{VT}

The vocal tract effect, subsequently applied by active control to the radiated impedance, is modelled by a causal stable linear time-invariant filter. This filter represents the formantic resonances applied to the airflows between the glottis and the lips. Its transfer function (up to the propagation delay) $H_{VT} \propto U_{mouth}/U_{glottis}$ is chosen as an all-pole filter in the Z-domain given by

$$H_{VT}(z) = \frac{G}{1 + \sum_{k=1}^{2K} a_k\, z^{-k}}, \tag{6}$$

where $G > 0$ is a gain. The coefficients a_k fix the poles of the filter (z_k assumed to be in $\mathbb{D}$ for stability and causality) and K (here, equal to 4) is the maximal number of formants (see e.g. [3, 4] and [5] for estimations based on LPC).

3. TARGET ACOUSTIC CONTROL

As mentioned in section 1, the target application is to produce a vocalised version of the radiated sound, by applying formants to the radiated pressure (3a) given the trombone airflow U_{tb}.

To this end, a controlled acoustic airflow (U_{ac}) is added to that of the trombone (U_{tb}) at the bell extremity ($U_R = U_{tb} + U_{ac}$). This control is assumed to be realised by an ideal source of flow in the low frequency range, defining the acoustic junction (see Fig. 3):

$$U_{tb} + U_{ac} = U_R, \tag{7a}$$

$$P_{ac} = P_R = P_{tb}. \tag{7b}$$

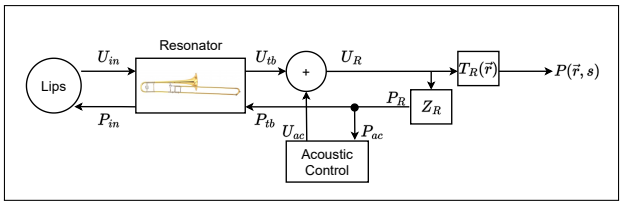

Figure 3. Block diagram of the acoustic control.

The control is designed such that the airflow (U_R) experienced by the natural acoustic radiation becomes a vocalised version of the trombone airflow ($H_{VT}U_{tb}$) rather than the trombone airflow itself (U_{tb}), that is (see Fig. 4)

$$U_R = H_{VT}U_{tb}. \tag{8}$$

Note that, from the trombone viewpoint, this amounts to loading its bell extremity by the modified radiation impedance $H_{VT}Z_R$, denoted Z_R^c below.

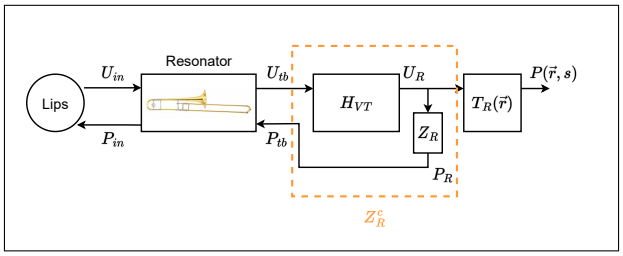

Figure 4. Block diagram of the target radiation impedance.

Then, modelling the acoustic control by its admittance $Y_{ac} = U_{ac}/P_{ac}$, it follows from (7a) that, at the acoustic junction,

$$U_{tb} + Y_{ac}P_{ac} = Z_R^{-1}P_R.$$

The expected target ($U_R = H_{VT}U_{tb}$) is achieved if $U_{tb} = H_{VT}^{-1}U_R = H_{VT}^{-1}Z_R^{-1}P_R$, so that this equation becomes

$$H_{VT}^{-1}Z_R^{-1}P_R + Y_{ac}P_{ac} = Z_R^{-1}P_R.$$

Finally, from (7b), the target acoustic control admittance is

$$Y_{ac} = Z_R^{-1}\left(1 - H_{VT}^{-1}\right). \tag{9}$$

4. ELECTRO-ACOUSTIC IMPLEMENTATION

To implement the acoustic control in practice, we use a loudspeaker located at $x = L$. Section 4.1 presents a brief reminder on its standard linear electro-acoustic modelling with Thiele and Small parameters [6, 7]. This loudspeaker is excited by means of a current generator assumed to be ideal on the frequency range of interest: note that the natural causal electric input of a loudspeaker is the voltage (and not the current) meaning that the current source requires the use of a dedicated feedback-loop circuit involving an operational amplifier (see e.g. [8]). Then (see Fig 5), the control current is governed by $I_{LS} = K\,V^{micro}$ where V^{micro} denotes the voltage delivered by a pressure microphone located at $x = L$. The transfer function K is the electronic control determined in section 4.2, in order to realise the acoustic target Y_{ac} given the loudspeaker model.

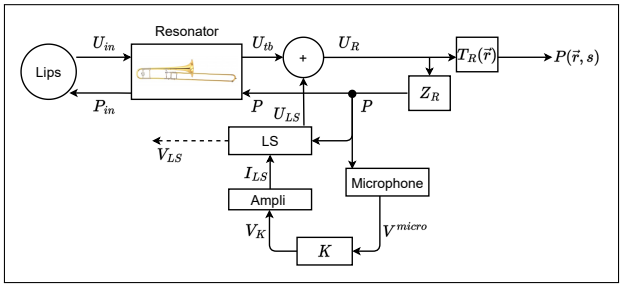

Figure 5. Diagram of the trombone equipped with the electroacoustic controller.

4.1 Loudspeaker modelling (Thiele and Small)

We briefly remind the electrical (10a) and mechanical (10b) equations that describe the model of Thiele and Small:

$$v_{LS}(t) = R_e i_{LS}(t) + L_e \frac{di_{LS}}{dt} + Bl\frac{dz}{dt}, \tag{10a}$$

$$M_m \frac{d^2 z}{dt} = Bl\, i_{LS}(t) - R_m \frac{dz}{dt} - \frac{1}{C_m} z(t) - S_d P, \tag{10b}$$

where M_m is the mass of the mobile loudspeaker equipment, R_m the mechanical resistance, C_m the mechanical compliance (suspension, spider, acoustic chamber) and S_d the equivalent surface area of the cone. Bl is the coefficient of the magnetic force induced by the current passing through the voice coil of length l. This model admits the following input (u) - state (x) - output (y) representation

Formants	Values
Bl	2.99 NA^{-1}
R_e	5.7 Ω
L_e	$1.1 \cdot 10^{-1}$ H
M_m	$1.9 \cdot 10^{-3}$ kg
R_m	$4.06 \cdot 10^{-1}$ Nm^{-1}
C_m	$5.4 \cdot 10^{-3}$ mN^{-1}

Table 1. Thiele and Small parameters of the speaker SICA 3L 0.8 SL 8Ω mode Z000900, given by the manufacturer.

$$\dot{x} = Ax + Bu, \qquad y = Cx, \tag{11a}$$

$$\text{with } u = \begin{pmatrix} v_{LS} \\ P \end{pmatrix}, \; x = \begin{pmatrix} i_{LS} \\ z \\ \dot{z} \end{pmatrix}, \; y = \begin{pmatrix} i_{LS} \\ U_{LS} \end{pmatrix}, \tag{11b}$$

$$A = \begin{pmatrix} -\frac{1}{\tau_e} & 0 & -\beta_e \\ 0 & 0 & 1 \\ \beta_m & -\omega_m^2 & -\frac{1}{\tau_m} \end{pmatrix}, \; B = \begin{pmatrix} \frac{1}{L_e} & 0 \\ 0 & 0 \\ 0 & \frac{S_d}{M_m} \end{pmatrix}, \tag{11c}$$

$$C = \begin{pmatrix} 1 & 0 & 0 \\ 0 & 0 & S_d \end{pmatrix}, \tag{11d}$$

and reduced parameters $\tau_e = \frac{L_e}{R_e}$, $\tau_m = \frac{M_m}{R_m}$, $\omega_m = \frac{1}{\sqrt{C_m M_m}}$, $\beta_e = \frac{Bl}{L_e}$, $\beta_m = \frac{Bl}{M_m}$, and where the output $U_{LS} \equiv U_{ac}$ denotes the airflow of the loudspeaker to be used for the acoustic control. Typical values used for simulations below are described in table 1.

4.2 Current control

This state-space representation describes a causal stable system, the transfer matrix of which is recalled in appendix A. However, as mentioned above, we consider here that the loudspeaker is controlled by a current source circuit (I_{LS}). In this case, expressing the position $Z(s)$ as $U_{LS}(s)/S_d$ in the Laplace domain (for zero initial condi-

tions), it straightforwardly follows from (10b) that

$$U_{LS}(s) = \tilde{A}_I(s)\, I_{LS}(s) + \tilde{A}_P(s)\, P(s), \tag{12a}$$

$$\tilde{A}_I(s) = \frac{s S_d Bl}{M_m s^2 + R_m s + \frac{1}{C_m}} = \frac{(S_d\, Bl/M_m)\, s}{s^2 + \frac{s}{\tau_m} + \omega_m^2}, \tag{12b}$$

$$\tilde{A}_P(s) = \frac{-S_d^2}{M_m s^2 + R_m s + \frac{1}{C_m}} = \frac{-S_d^2/M_m}{s^2 + \frac{s}{\tau_m} + \omega_m^2}. \tag{12c}$$

Their expressions in the Z-domain (detailed hereafter in (15a-15b)), called A_I and A_P, are calculated using the bilinear transform as a numerical scheme that preserves the stability of the filters, namely,

$$s = S(z) = 2 f_s \frac{1 - z^{-1}}{1 + z^{-1}}.$$

Now, we assume that the microphone and the amplifier (current source) are simple gains G_{micro} and G_{ampli}, and we renote $K(z)$ the transfer function $G_{ampli}\, K(z)\, G_{micro}$ from $P(s)$ to $I_{LS}(z)$ in the Z-domain, for conciseness. Then, according to Fig. 5 and (12a), it follows that (in the Z-domain)

$$\begin{aligned} U_{LS} &= A_I\, I_{LS} + A_P\, P \\ &= (A_I K + A_P)\, P. \end{aligned} \tag{13}$$

Finally, from (7a) with $U_{ac} = U_{LS}$, the radiated airflow is given by $U_R = U_{tb} + (A_I K + A_P)\, Z_R U_R$, so that by identification with (8), the transfer function of the target control is

$$K = A_I^{-1} \left[Y_R (1 - H_{VT}^{-1}) - A_P \right]. \tag{14}$$

5. NUMERICAL RESULTS

5.1 Description of experiments

This section introduces two numerical experiments intended to simulate the model of active trombone previously described. In the first (E1), the trombone is driven by a swept-sine. In the second, it is driven by a flow rate waveform measured in real trombone mouthpiece while playing a $B\flat_2$ [9].

The $(a_k)_{k\in[1,N]}$ coefficients of the vocal tract transfer function, see equation (6), are deduced from its N pairs of conjugated poles, themselves estimated using LPC analysis [5] from the first N formants of the vocal tract. Indeed, each formant of frequency f_k^{res} and Q factor Q_k introduces the pair of poles $\rho_k e^{\pm i\theta_k}$, $k \in [1, N]$, with:

Formants	1	2	3	4
f_k^{res} (Hz)	551	944	1928	2835
Q_k ($\times 10^{-1}$)	0.79	1.4	4.7	4.9

Table 2. Frequencies and Q-factors of the resonances of a vocal tract while pronouncing a vowel [A], calculated from the poles estimated by LPC analysis, with a sample rate of 8 kHz.

$$\rho_k = e^{\frac{-\pi f_k^{res}}{Q_k F_s}} \text{ and } \theta_k = \frac{2\pi f_k^{res}}{F_s} \sqrt{1 - \frac{1}{4Q_k^2}} \tag{16}$$

In these expressions, F_s is the sample rate used for the simulation.

For a given target vocal tract, the pole characteristics given by LPC analysis, noted ρ_k^{LPC} and θ_k^{LPC}, are *a priori* calculated with another sample rate, called F_s^{LPC}. Consequently, the pole characteristics used in H are, $\forall k \in [1, N]$:

$$\begin{aligned} \rho_k &= (\rho_k^{LPC})^{\frac{F_s^{LPC}}{F_s}} \\ \text{and } \theta_k &= \theta_k^{LPC} \times \frac{F_s^{LPC}}{F_s} \end{aligned}$$

As an example, the transfer function of a vocal tract while pronouncing the vowel [A] is calculated from its first four pairs of conjugated poles, which are estimated using LPC analysis, cf Fig. 6. As expected, its modulus shows four resonances. The corresponding frequencies f_k^{res} and Q factors Q_k are calculated using equation (16) and listed in Table 2.

5.2 Time-domain results

In order to validate the model of active trombone previously described, we simulate the waveforms of pressure and of radiated flow at the bell extremity as well as the mouthpiece pressure, for a given mouthpiece flow called U_{in}, as shown in Fig.4. These calculations rely on the transfer functions $\frac{U_{tbn}}{U_{in}}^i$, $\frac{P}{U_{in}}^i$ and $\frac{P_{in}}{U_{in}}^i$ derived from (1b):

$$\left(\frac{U_{tb}}{U_{in}}\right)^i = \frac{2\, z^{-N}}{1 + \frac{Z_R^i}{Z_c} + \left(1 - \frac{Z_R^i}{Z_c}\right) z^{-2N}} \tag{17}$$

$$\left(\frac{P_{tb}}{U_{in}}\right)^i = \frac{2\, Z_R^i\, z^{-N}}{1 + \frac{Z_R^i}{Z_c} + \left(1 - \frac{Z_R^i}{Z_c}\right) z^{-2N}} \tag{18}$$

$$A_I(z) = -2f_s S_d Bl \frac{z^{-2}-1}{z^{-2}[4f_s^2 M_m - 2f_s R_m + 1/C_m] + z^{-1}[-8f_s^2 M_m + 2/C_m] + 4f_s^2 M_m + 2f_s R_m + 1/C_m} \quad (15a)$$

$$A_P(z) = -S_d^2 \frac{z^{-2}+2z^{-1}+1}{z^{-2}[4f_s^2 M_m - 2f_s R_m + 1/C_m] + z^{-1}[-8f_s^2 M_m + 2/C_m] + 4f_s^2 M_m + 2f_s R_m + 1/C_m} \quad (15b)$$

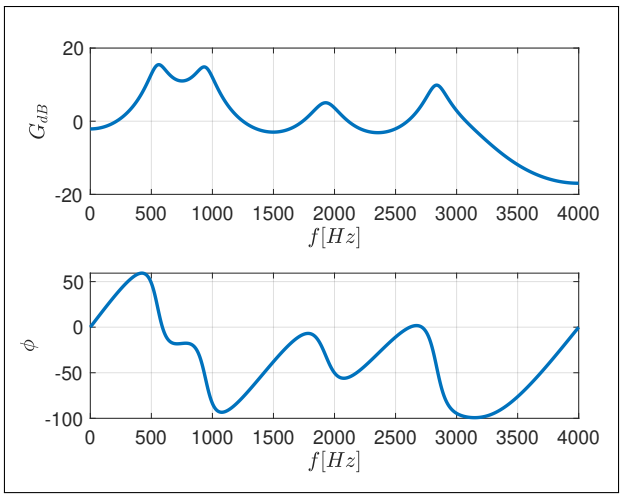

Figure 6. Modulus (top) and phase (bottom) of vocal tract transfer function while pronouncing the vowel [A].

$$\left(\frac{P_{in}}{U_{in}}\right)^i = \frac{Z_R^i + Z_c + (Z_R^i - Z_c)z^{-2N}}{1 + \frac{Z_R^i}{Z_c} + \left(1 - \frac{Z_R^i}{Z_c}\right)z^{-2N}} \quad (19)$$

where $i = c$ in the presence of control or $i = \emptyset$ in the absence of control. We note that (17), (18) and (19) are causal, even when the control is on.

5.3 Frequency-domain results

The waveforms calculated in 5.2 are not shown in the paper, but are used to determine the effect of active control on the radiation impedance and the input impedance of the trombone for both driving signals (E1) and (E2). For that purpose, we compute the ratio between the Fourier transforms of P_{in} and U_{in} on the one hand, and of P and U_{tbn} on the other hand, and compare them to Z_{in} and Z_R, in the presence and in the absence of control.

Fig. 7 corresponds to the (E1)-experiment.

- We compute $Z_R^\emptyset = \rho_0 c_0 / S_R$ and we compare with the calculation of the ratio (P without control from (18) / (U_{tbn} without control from (17)).
- We compute $Z_{in}^\emptyset$ from (4b) with $Z_R^\emptyset$ and we compare it with the ratio (P_{in} without control from (19))/(U_{in} without control from (17)).

The results of this calculations are shown on the first column.

- We compute $Z_R^c = H_{VT}\rho_0 c_0 / S_R$ and we compare it with the ratio (P with control from (18))/(U_{tbn} with control from (17).
- We compute Z_{in}^c from (4b) by using Z_R^c and we compare it with the ratio (P_{in} with control)/(U_{in} with control).

The results are shown on the second culumn. The third column is deduced from the culumns 1 and 2.

Also, as expected, the graphs of Z_R^i do not depend on frequency. For $Z_R^\emptyset$, we chose to represent the ratio $Z_R^\emptyset/(\rho_0 c_0/S_R)$.In the presence of control (middle bottom of Fig. 7), Z_R^c shows the formantic envelope H_{VT} translated upwards by $20 \times \log\left(\frac{\rho_0 c_0}{S_R}\right) \approx 111$. And as expected, the ratio $Z_R^c/Z_R^\emptyset$, cf. Fig. 7), bottom right, is equal to the formantic envelope H_{VT}.

Fig. 8 corresponds to the (E2)-experiment. The calculation method is the same as for the (E1)-experiment but with a measured flow (see [10]). This is what gives Fig. 8. Even if the majority of the measurement ranges from 40 to 1800 Hz, we present the results up to 4000 Hz since the vocal formants of an [A] vowel extend up to 3000 Hz (see Table 2). The results concerning the radiation impedance remain good. The variations around the expected value for $Z_R^\emptyset$ are of the order of less than 10^{-11} dB. However, the signal is noisy, since we start from a recorded experimental signal.

6. CONCLUSION AND PERSPECTIVES

This brief analysis has provided first theoretical results of the radiation impedance control of a trombone. Numerical results have shown that it is possible to radiate a vowel

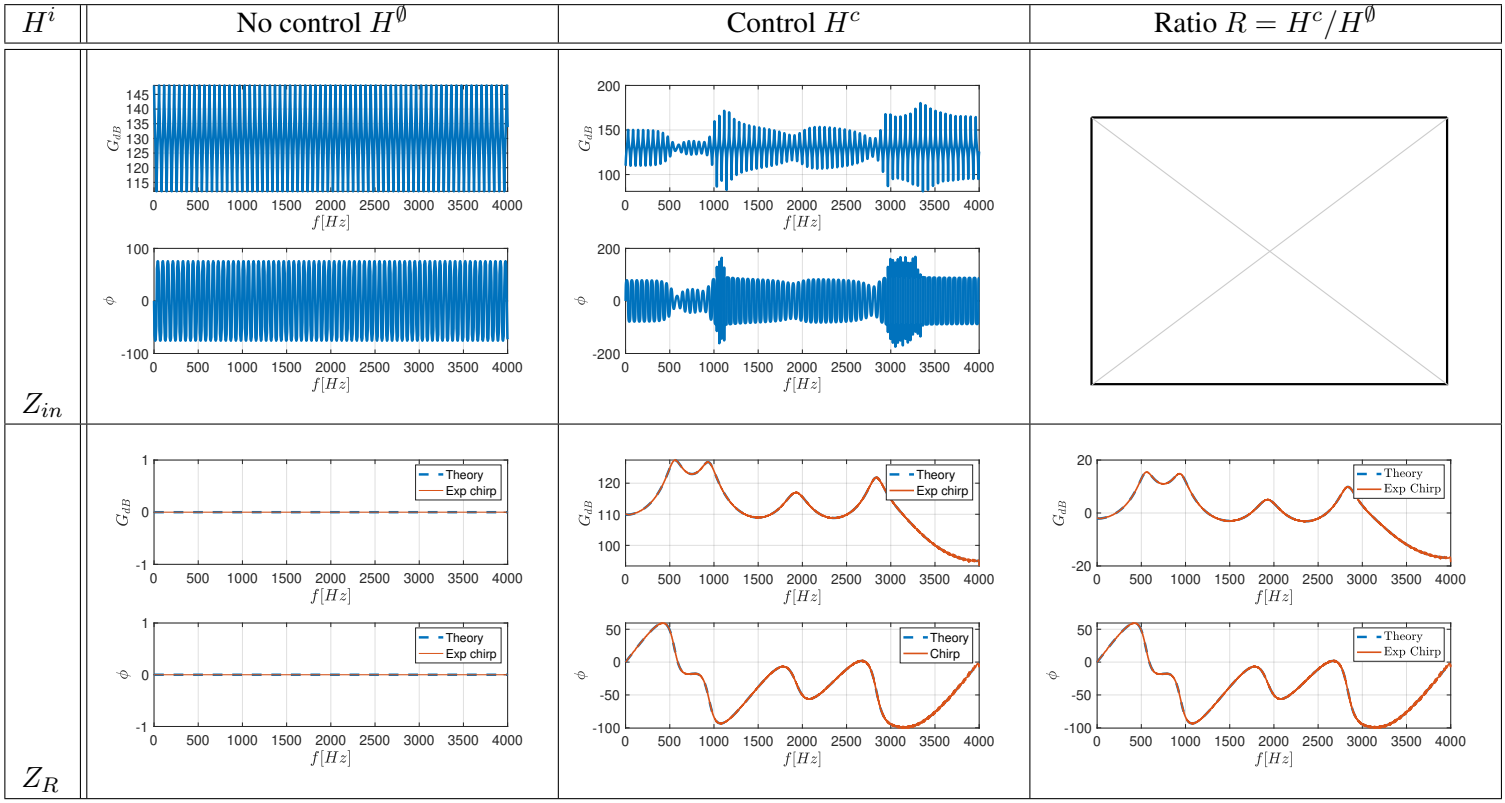

Figure 7. (E1) Transfer functions H^i in the Fourier domain, with ($i = c$) and without ($i = \emptyset$) control: (solid lines) computed from theoretical z-transforms with $z = \exp(2i\pi f/f_s)$; (dotted line) computed from the FFT of the pressure and flow waveforms.

within the instrument by modulating the natural flow of the trombone through the vocal tract formants associated with a fixed vowel. The model presented in this article remains only under Time-Linear Invariant assumptions. No non-linearity has been studied. Some techniques such as Port-Hamiltonian Systems (PHS) [11] provide a suitable starting point to treat the non-linearities of the model.

A. TRANSFER MATRIX OF THE LOUDSPEAKER

In the Laplace domain, the input-to-output relation $Y(s) = \tilde{H}(s)U(s)$ is given by the transfer matrix $\tilde{H}(s) = C(s\,I_3 - A)^{-1}B$, which is equal to

$$\tilde{H}(s) = \frac{1}{\Delta(s)} N(s), \tag{20a}$$

$$N(s) = \begin{pmatrix} \left(s^2 + \frac{s}{\tau_m} + \omega_m^2\right)\frac{1}{L_e} & s\,\gamma \\ s\,\gamma & \left(s^2 + s\,\frac{1}{\tau_e}\right)\frac{S_d^2}{M_m} \end{pmatrix}, \tag{20b}$$

$$\Delta(s) = \sum_{k=0}^{3} \delta_k s^k, \tag{20c}$$

with $\delta_0 = \frac{\omega_m^2}{\tau_e}$, $\delta_1 = \omega_m^2 + \frac{1}{\tau_e \tau_m} + \beta_e\beta_m$, $\delta_2 = \frac{1}{\tau_e} + \frac{1}{\tau_m}$, $\delta_3 = 1$, and $\gamma = \frac{\beta_e\beta_m S_d}{Bl} = \frac{Bl\,S_d}{L_e\,M_m}$.

B. REFERENCES

[1] V. Martos, H. Boutin, T. Hélie, and B. d'Andrea Novel, "Contrôle actif de résonateur de cuivre: approche linéaire avec transducteurs co-localisés," in 16ème Congrès Français d'Acoustique, CFA2022, 2022.

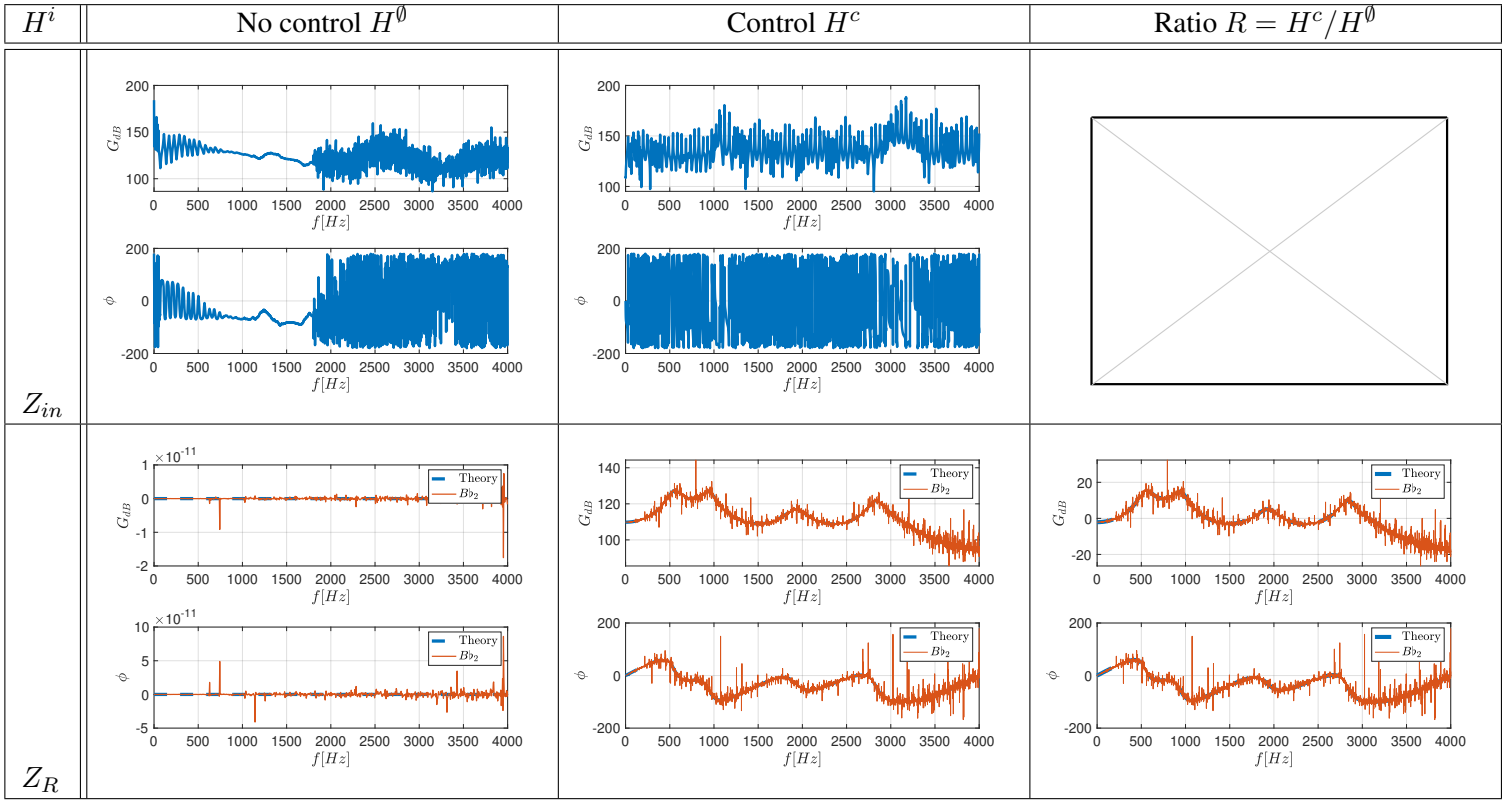

Figure 8. (E2) Transfer functions H^i in the Fourier domain, with ($i = c$) and without ($i = \emptyset$) control: (solid lines) computed from theoretical z-transforms with $z = \exp(2i\pi f/f_s)$; (dotted line) computed from the FFT of the time-domain input and output signals.

[2] A. Chaigne, Ondes acoustiques. Paris: Ecole Polytechnique, 2003.

[3] J. D. Markel and A. J. Gray, Linear prediction of speech, vol. 12. Springer Science & Business Media, 2013.

[4] I. R. Titze and D. W. Martin, Principles of voice production. Acoustical Society of America, 1998.

[5] T. Hélie, Vocoder par LPC. Paris: Mines ParisTech, 2012.

[6] N. Thiele, "Loudspeakers in vented boxes : Part 1," Journal of the Audio Engineering Society, p. 382–392, 1971.

[7] R. Small, "Closed-box loudspeaker systems-part 1 : analysis," Journal of the Audio Engineering Society 20, p. 798–808, 1972.

[8] A. P. McPherson, "Techniques and circuits for electromagnetic instrument actuation.," in NIME, London, 2012.

[9] H. Boutin, N. Fletcher, J. Smith, and J. Wolfe, "Relationships between pressure, flow, lip motion, and upstream and downstream impedances for the trombone," The Journal of the Acoustical Society of America, vol. 137, no. 3, pp. 1195–1209, 2015.

[10] H. Boutin, Méthodes de contrôle actif d'instruments de musique. Cas de la lame de xylophone et du violon. PhD thesis, UPMC-Université Paris 6 Pierre et Marie Curie, 2011.

[11] B. Maschke, A. V. D. Schaft, and P. C. Breedveld, "An intrinsic hamiltonian formulation of network dynamics: Non-standard poisson structures and gyrators," Journal of the Franklin institute, vol. 329, no. 5, pp. 923–966, 1992.